

Supporting Information

To catalyze or not to catalyze: Elucidation of the subtle differences between the hexameric capsules of pyrogallolarene and resorcinarene

Qi Zhang,^a Lorenzo Catti,^a Ville R.I. Kaila,^c Konrad Tiefenbacher^{a,b*}

^a Department of Chemistry, University of Basel, St. Johannisring 19, CH-4056
Basel, Switzerland

^b Department of Biosystems Science and Engineering, ETH Zürich, Mattenstrasse
26, CH-4058 Basel, Switzerland

^c Department of Chemistry, Technical University of Munich, Lichtenbergstrasse
4, 85747 Garching, Germany.

E-mail: konrad.tiefenbacher@unibas.ch / tkonrad@ethz.ch

Table of Contents

1. General information	3
2. Binding studies with tertiary amines.....	8
2.1 ¹ H-NMR titration with triethylamine (5a)	8
2.2 DOSY-experiments of pyrogallolarene capsule II	10
2.3 Comparison of trialkylamines (5a-d).....	12
3. Binding studies with tetraalkylammonium salts	13
3.1 Comparison of tetraalkylammonium bromides (6a-d⁺Br⁻)	13
3.2 Investigations concerning the precipitate formed with Et ₄ N ⁺ Br ⁻ (6a⁺Br⁻)....	16
3.3 Encapsulation studies with ethyltripropylammonium mesylate (6e⁺MeSO₃⁻)	18
4. Catalysis attempts with pyrogallolarene capsule II	25
4.1 Procedure for cyclization reactions.....	25
4.2 Determination of the pK _a value of pyrogallolarene II	26
4.3 Catalysis attempts with additional external acids	29

5. Quantum chemical calculations	29
6. ESP surface map of capsule I and II	31
7. References.....	32
8. NMR spectra for new compounds	33

1. General information

Experimental. Reactions were carried out under an atmosphere of argon, unless otherwise indicated. ^1H -NMR and ^{13}C -NMR spectra were recorded at 500 MHz and 126 MHz respectively, using a Bruker AV 500 spectrometer. ^1H -NMR and ^{13}C -NMR chemical shifts (measured at 298 K, unless otherwise stated) are given in ppm by using CHCl_3 and CDCl_3 as references (7.26 ppm and 77.16 ppm, respectively). Coupling constants (J) are reported in Hertz (Hz). Standard abbreviations indicating multiplicity were used as following: s (singlet), t (triplet), q (quartet) and m (multiplet). 2D-DOSY spectra were recorded with a Bruker AV 500 spectrometer using the Bruker standard DOSY routine. GC-analysis was performed with an Agilent GC6890 instrument equipped with a FID detector and a HP-5 capillary column (length = 29.5 m). Hydrogen was used as the carrier gas and the constant-flow mode (flow rate = 1.8 mL/min) with a split ratio of 1:20 was used.

Source of chemicals. Tetrabutylammonium bromide and tetrapropylammonium bromide were purchased from Acros Organics. CDCl_3 was purchased from Deutero GmbH. Dodecanal, trihexylamine and resorcinol were purchased from Alfa Aesar. Triethylamine and pyrogallol were purchased from Merck KGaA. Tetraethylammonium bromide, Tetrahexylammonium bromide, tributylamine and tripropylamine were purchased from Sigma-Aldrich. Ethanol (99.9%) was purchased from VWR. All chemicals were used as received, unless otherwise stated. Methanol and diethyl ether were purchased from Brenntag and distilled prior to use. Sonication was performed in a VWR Ultrasonic Cleaner USC-300TH. Transfer of liquids with a volume ranging from 1 to 10 μL or from 10 to 100 μL was performed with a microman M1 pipette (Gilson) equipped with 10 μL or 100 μL pipette tips, respectively.

Resorcinarene **1**¹ and trioctadecylamine **7**² were synthesized according to literature procedures.

Pyrogallolarene **2** was synthesized according to a literature procedure³: To a stirring solution of 99.9% ethanol (60 mL) and 37% aqueous HCl (14 mL), pyrogallol (11.4 g, 90.0 mmol, 1.0 eq) was added. After the solution was cooled to 0 °C, a solution of dodecanal (20.0 mL, 90.0 mmol, 1.0 eq) in 99.9% ethanol (10 mL) was added slowly into the reaction mixture over 15 min. The resulting solution was allowed to warm to 25 °C slowly and was then refluxed at 100 °C for 24 h. Afterwards, the reaction mixture was cooled to room temperature, and the formed precipitate was filtered and washed with ethanol (120 mL). Air was drawn through the precipitate for 20 min (aspirator). The solid was recrystallized from ethanol (50 mL) and air was drawn through the precipitate for 20 min (aspirator). The obtained crystalline material was then dried by utilizing a rotary evaporator (50 °C and 4 mbar), until the residual ethanol was removed completely. Compound **2** (18.3 g, 63.0 mmol, 70%) was obtained as an off-white crystalline solid.

Preparation of host stock solution: CDCl₃ (ca. 80% of the capacity of the volumetric flask) was added to **1** or **2** in a volumetric flask and the sample was homogenized by sonication, gentle heating with a heat gun and agitation to give a clear solution. The volumetric flask was filled up to the calibration mark with CDCl₃ and again homogenized by agitation to give a solution with a concentration as given in *SI-Table 1*.

SI-Table 1: Preparation of host stock solution.

	molecular weight (g/mol)	mass (mg)	volumetric flask (mL)	concentration (mmol/L)
resorcinarene 1	1106	140	2.00	63.3
pyrogallolarene 2	1170	295	5.00	50.4

Preparation of guest stock solution: Stock solutions of guests were prepared with a concentration of 83.3 mmol/L in CDCl₃.

Sample preparation: To the host solution (159 μL for **1** and 198 μL for **2**, 10.0 μmol , 6.0 eq) in a NMR-tube was added CDCl_3 (320 μL for **1**, 280 μL for **2**) and guest stock solution (20 μL , 1.67 μmol , 1.0 eq). The sample was homogenized by agitation. All experiments were conducted in triplicate and the average values including standard deviation are reported. NMR spectra were recorded at least 3 h after sample preparation to make sure protonation and/or encapsulation equilibria were reached.

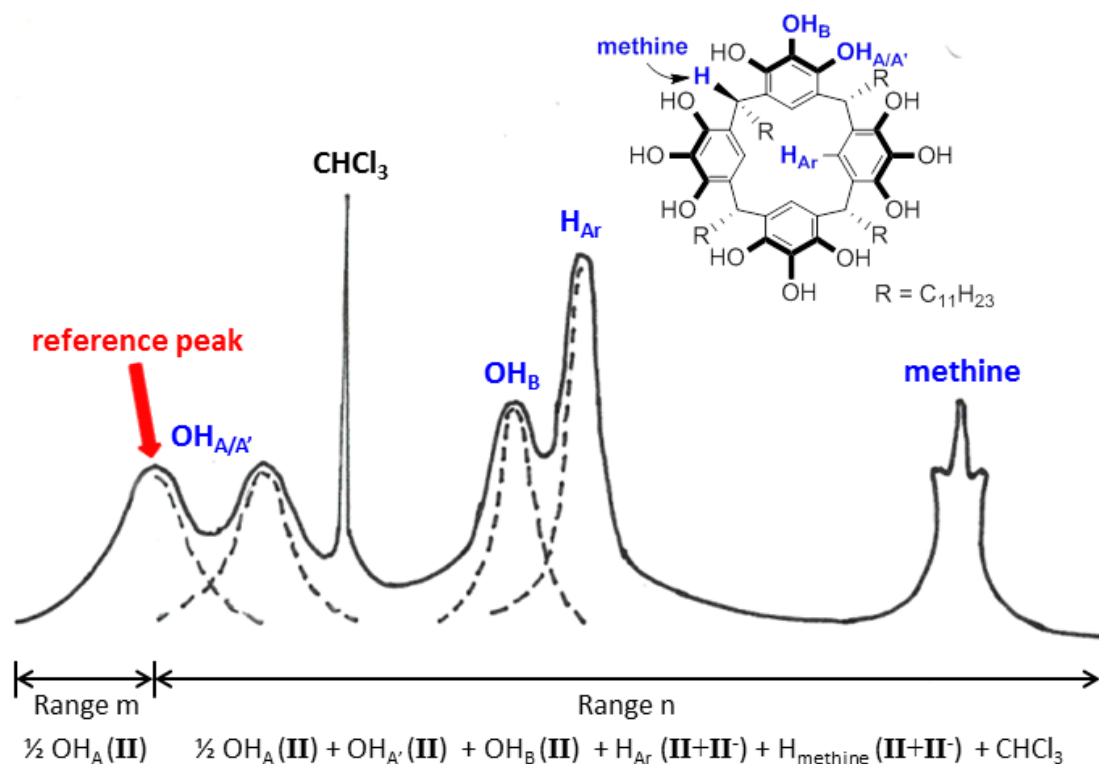
Determination of the encapsulation ratio: In case of binding studies, the integral of the methine group (4.29 ppm for **1** and 4.37 ppm for **2**, t, $J = 7.7$ Hz, 24H) of capsule **I** or **II** was used as the reference. In case of experiments with NEt_3 (**5a**) and $\text{Et}_4\text{N}^+\text{Br}^-$ (**6a** $^+\text{Br}^-$), the terminal methyl groups appearing between 0 and -1 ppm after encapsulation were utilized for calculating the encapsulation ratio. For more bulky guests, it's elusive how many of the respective alkyl groups are shifted into the negative ppm range due to the anisotropic effect of capsule walls. Therefore, the encapsulation degree of such guests was determined by comparing the integral of the remaining methylene groups adjacent to the nitrogen atoms in tertiary amines **5** or tetraalkylammonium bromides **6** $^+\text{Br}^-$ to their original values (6H for **5** or 8H for **6** $^+\text{Br}^-$, highlighted with an asterisk * in the corresponding spectra). It is noteworthy that both methods yielded comparable values of encapsulation ratio for **5a** ($44 \pm 2\%$ determined by the terminal methyl groups between 0 and -1 ppm, $47 \pm 1\%$ determined by the remaining methylene groups).

Determination of the deprotonation ratio: Depending on the deprotonation degree of the pyrogallolarene capsule **II**, the calculation of the deprotonation ratio was divided into three cases:

a) Little deprotonation: the broad peak of the phenol signals of **II** $^-$ and water remained in the high-field range. The low field phenol peak of **II** (9.40 – 8.40 ppm, m, 24H, 'reference peak') was used for determining the amount of deprotonation, since it does

not overlap with other signals. The ratio of deprotonation was directly determined by comparing the integral of the remaining phenolic protons to its original value (24H). This method is applicable for the experiment with imidazol (1 eq, see SI–Fig. 16)

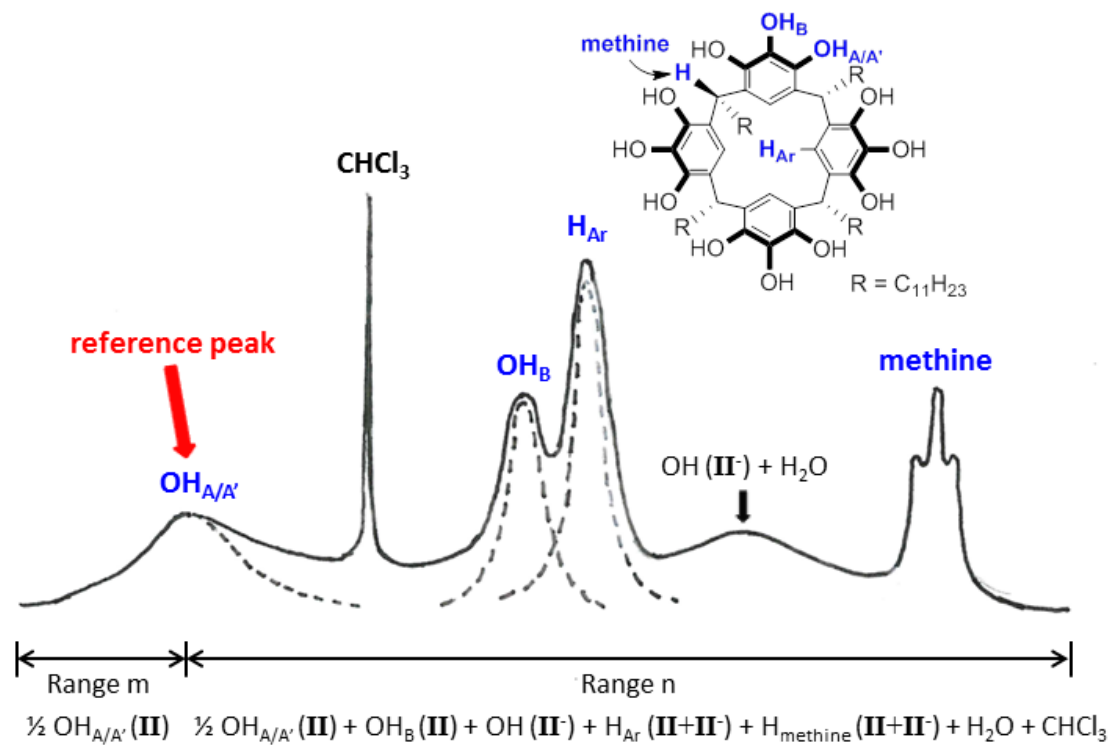
b) As more deprotonation occurs, the broad peak (phenol signals of II^- and water) experienced some down–field shift but still remained < 4 ppm. All phenolic peaks became broad. The right half of the ‘reference peak’ overlaps with the neighboring phenol signal. The deprotonation degree was determined by comparing the integral of the left half of the reference peak (OH_A or $\text{OH}_{A'}$) to its original value (12H) as shown in *SI–Scheme 1*. This method is applicable for the experiments with NEt_3 (0.5 – 0.7 eq), DABCO (1 eq) and morpholine (1 eq).



SI–Scheme 1: Determination of deprotonation ratio according to method **b**.

c) At high deprotonation ratios (ca. $\geq 25\%$), the ‘reference peak’ and the neighboring phenolic group merge into a single broad peak. The broad peak corresponding to phenol signals of II^- and water signals, shifts into the down–field region and overlaps with signals of II . The deprotonation degree is determined by comparing the integral

of the left half of the reference peak (OH_A and $\text{OH}_{A'}$) to its original value (24H) as described in *SI-Scheme 2*. This method is applicable for the experiment with NEt_3 (0.8–1.0 eq) and DMAP (1 eq).



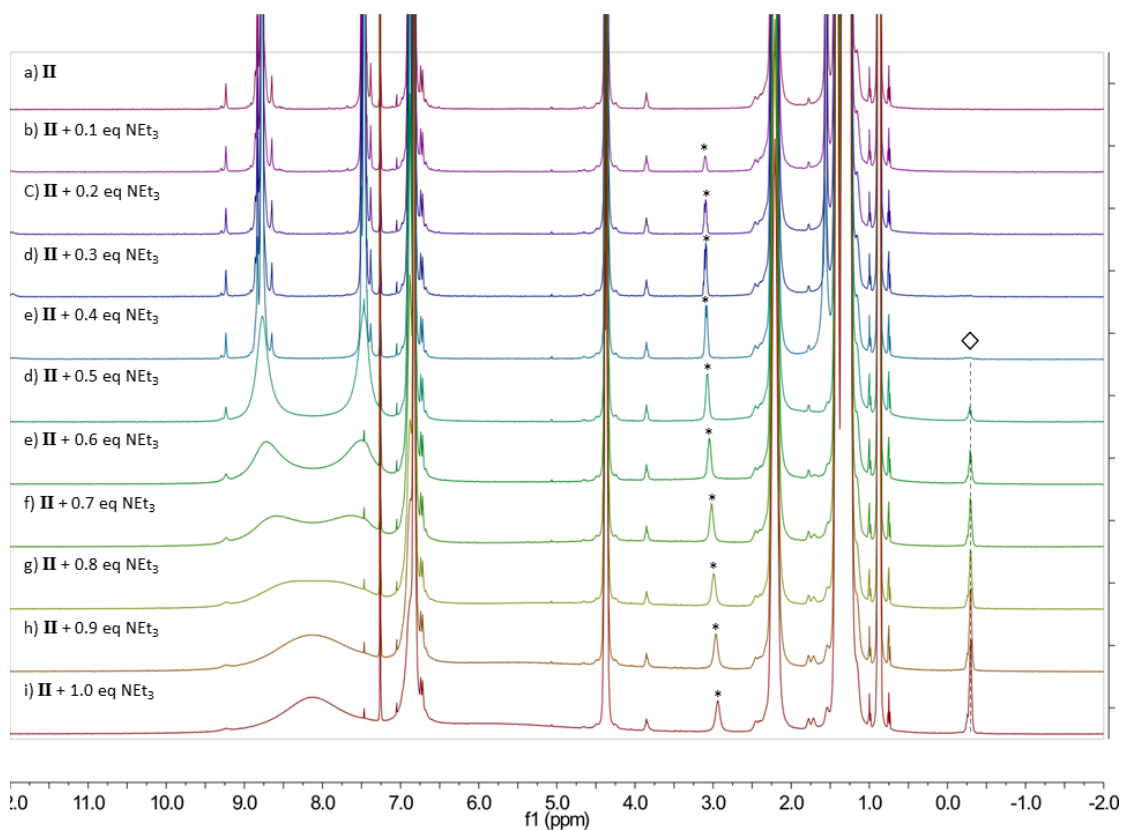
SI-Scheme 2: Determination of deprotonation ratio according to method **c**.

The validity of methods **b** and **c** was verified in the titration experiment of pyrogallolarene capsule **II** with NEt_3 (*SI-Table 2*) by comparing the calculated integrals in range **n** with the determined ones.

2. Binding studies with tertiary amines

2.1 ^1H -NMR titration with triethylamine (5a)

To the stock solution of pyrogallolarene **2** (198 μL , 11.7 mg, 10.0 μmol , 6.0 eq) in a NMR-tube was added NEt_3 -stock solution with a concentration of 8.4 mmol/L (a multiple of 20 μL , 0.167 μmol , 0.1 eq.). Then the sample was diluted with CDCl_3 to a volume of 0.50 mL, to obtain a sample of the desired **II**/ NEt_3 -ratio. After agitation the sample was allowed to equilibrate for $\geq 3\text{h}$ and then subjected to NMR-spectroscopy.



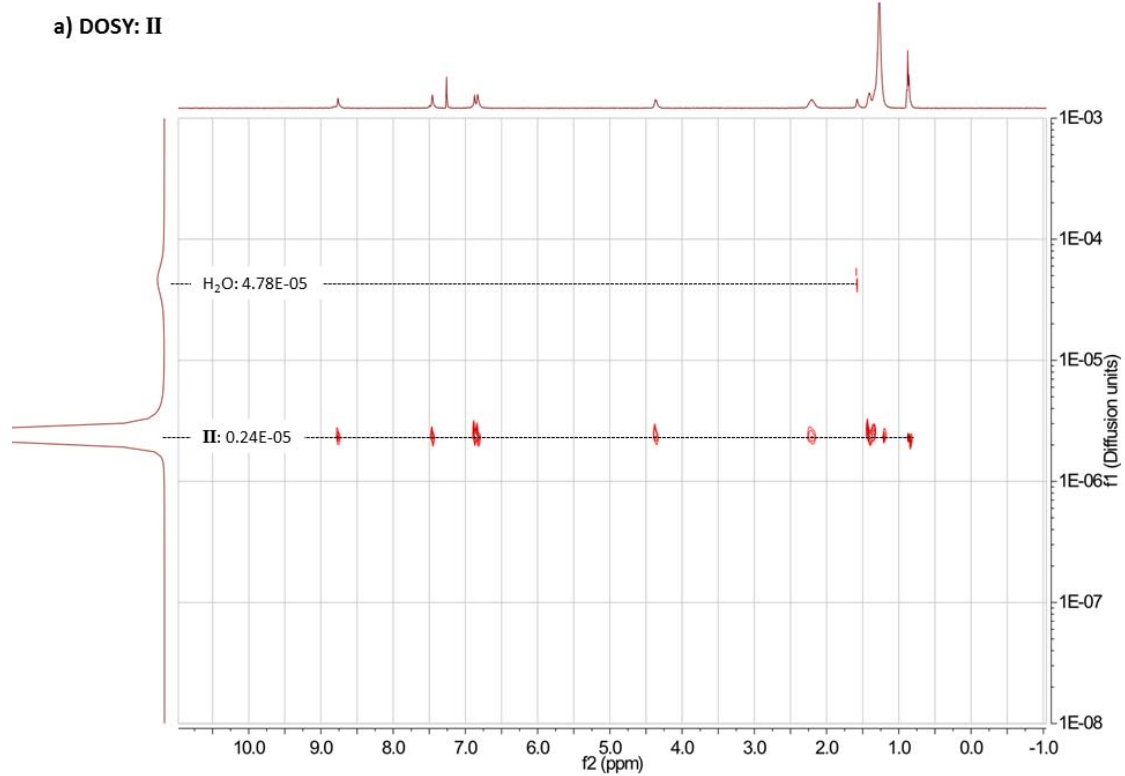
SI-Figure 1: ^1H -NMR titration of capsule **II** (a) in CDCl_3 (3.3 mM) with various amounts of NEt_3 (b-i). Signals corresponding to free and encapsulated guest are highlighted by an asterisk and a square, respectively.

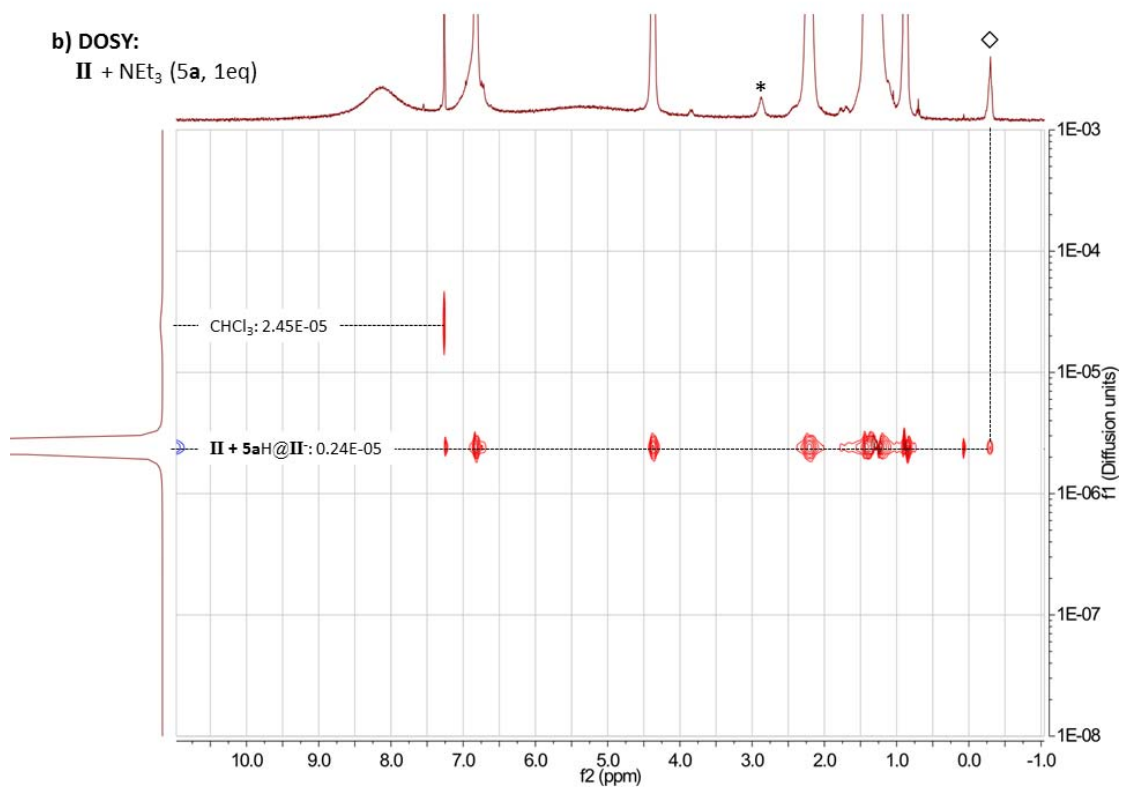
Deprotonation ratios of **II** were determined by method **b** or **c** described in **SI-Scheme 1** or **2**, respectively. The measured integrals in range **n** have a good correlation with the calculated values (see, **SI-Table 2**).

SI-Table 2: Titration experiment of **II** with NEt₃. The methine peak (24H) was utilized as reference for integration. Integrals of H₂O (12.7H) and CHCl₃ (6.0H) were determined in a blank sample (entry 0). nd = not detectable.

entry	II/NEt ₃	encapsulation ratio	Range n		deprotonation	
			calc.	measured	method	ratio
0	1:0			—		
1	1:0.1	0%				
2	1:0.2	2%		nd	nd	nd
3	1:0.3	4%				
4	1:0.4	6%				
5	1:0.5	10%	110.8	111.6	b	5%
6	1:0.6	22%	109.0	110.9	b	8%
7	1:0.7	28%	106.8	105.0	b	12%
8	1:0.8	37%	118.5	118.9	c	16%
9	1:0.9	40%	120.0	119.0	c	22%
10	1:1.0	45%	121.5	121.3	c	29%

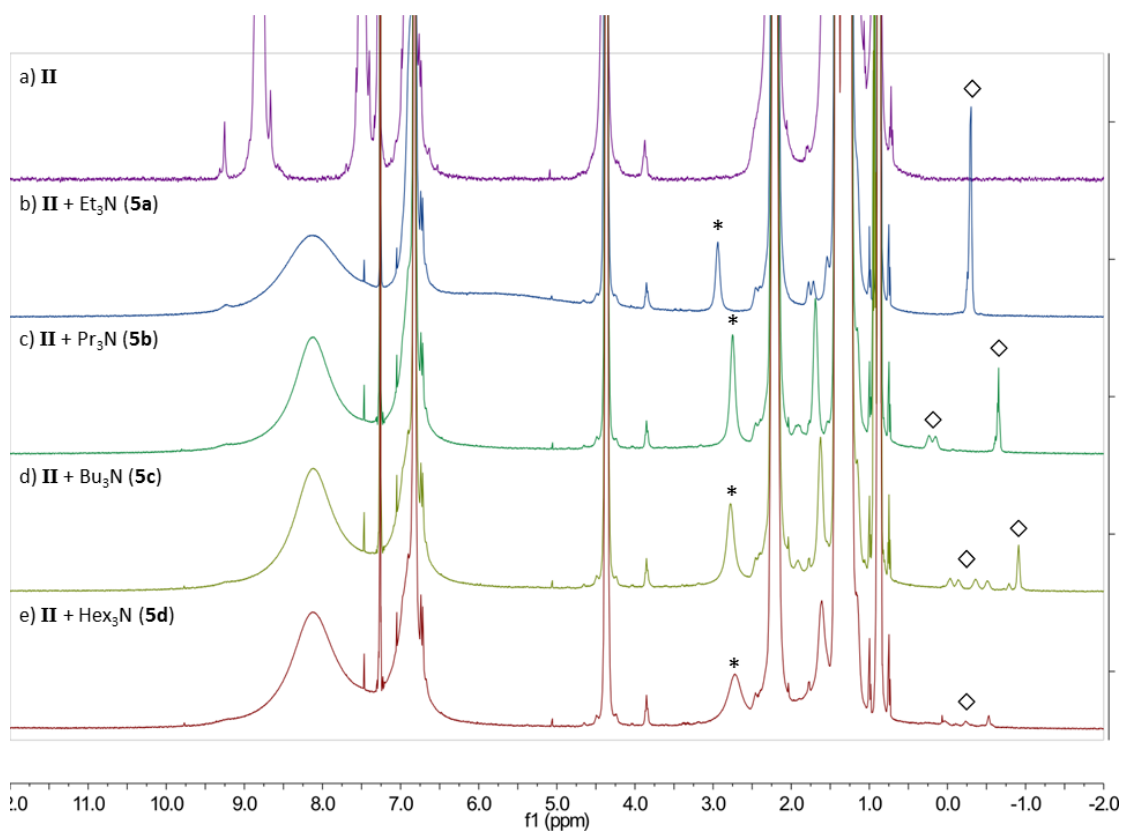
2.2 DOSY-experiments of pyrogallolarene capsule II





SI-Figure 2: DOSY spectra of pyrogallolarene capsule **II**. The diffusion coefficients are given in cm²/s. a) **II** (3.3 mM); b) **II**/NEt₃ = 1/1, **II** (3.3 mM), NEt₃ (3.3 mM). Signals corresponding to free and encapsulated guest are highlighted by an asterisk and a square, respectively.

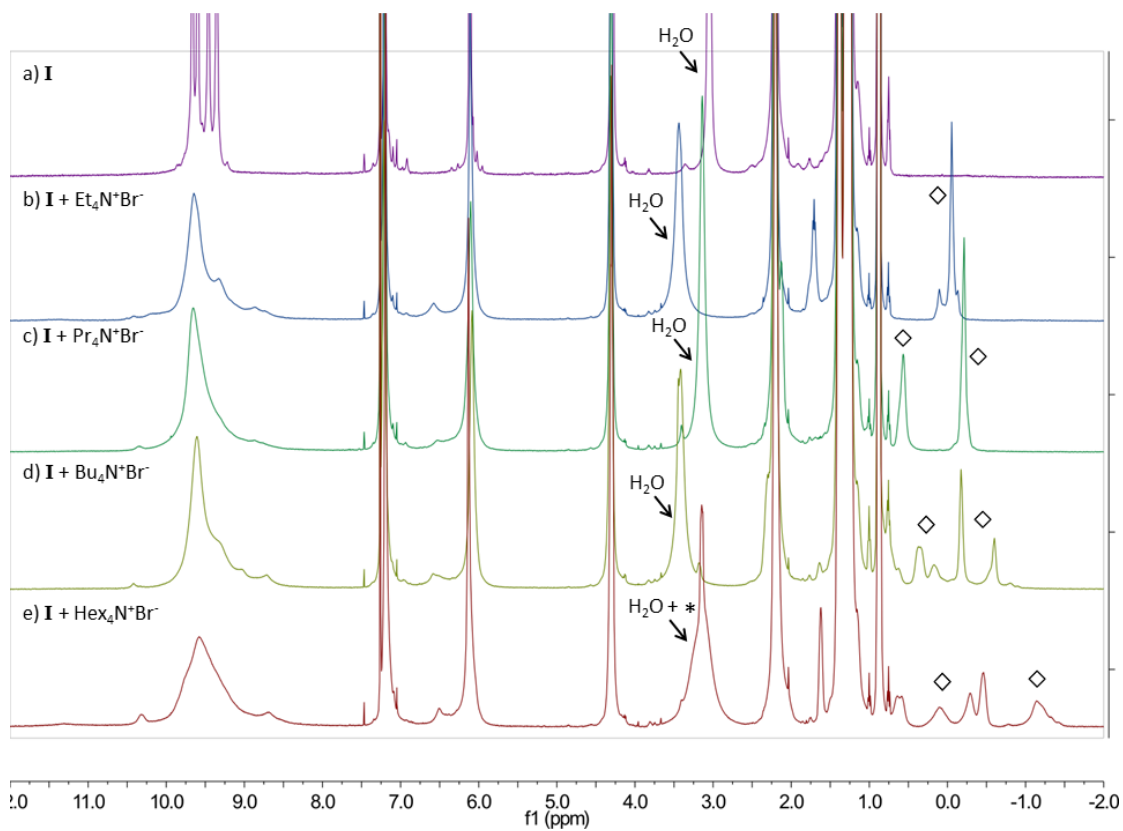
2.3 Comparison of trialkylamines (5a–d)



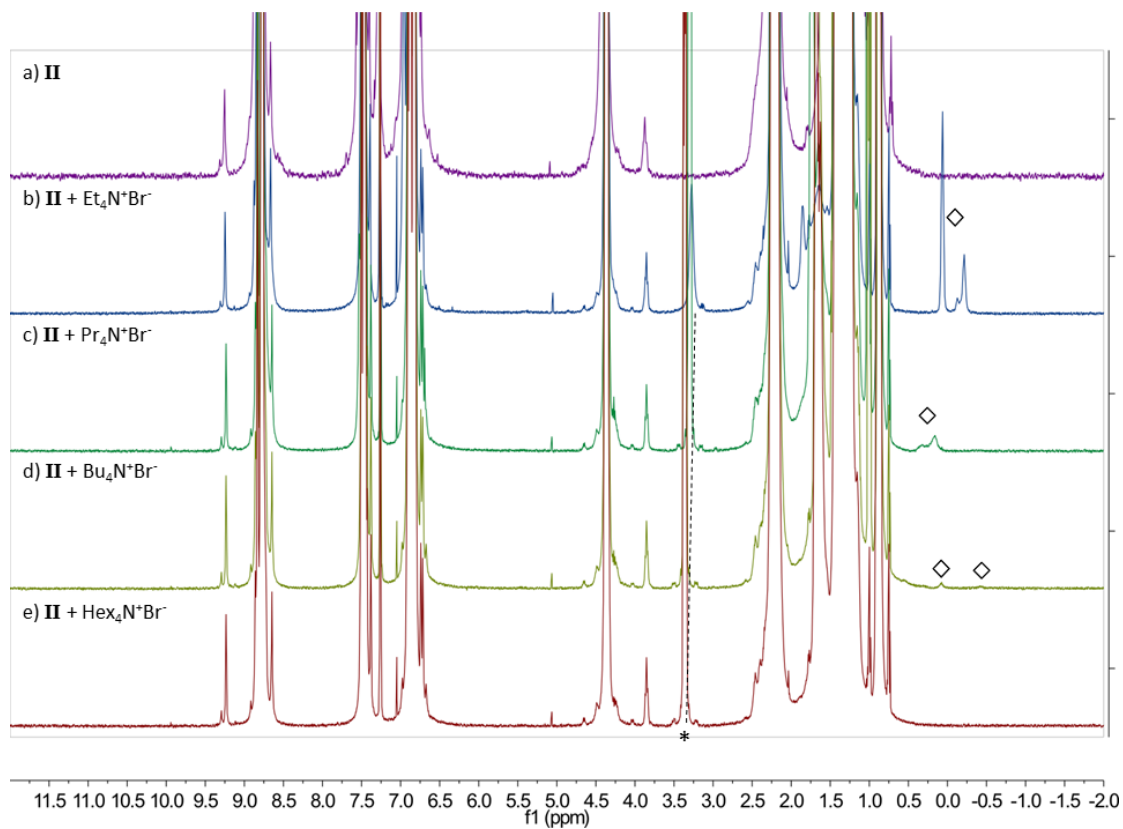
SI-Figure 3: Binding and deprotonation studies of pyrogallolarene capsule **II**. a) **II** (3.3 mM), with b) Et₃N (**5a**) (3.3 mM); c) Pr₃N (**5b**) (3.3 mM); d) Bu₃N (**5c**) (3.3 mM); e) Hex₃N (**5d**) (3.3 mM). Signals corresponding to free and encapsulated guest are highlighted with an asterisk and a square, respectively.

3. Binding studies with tetraalkylammonium salts

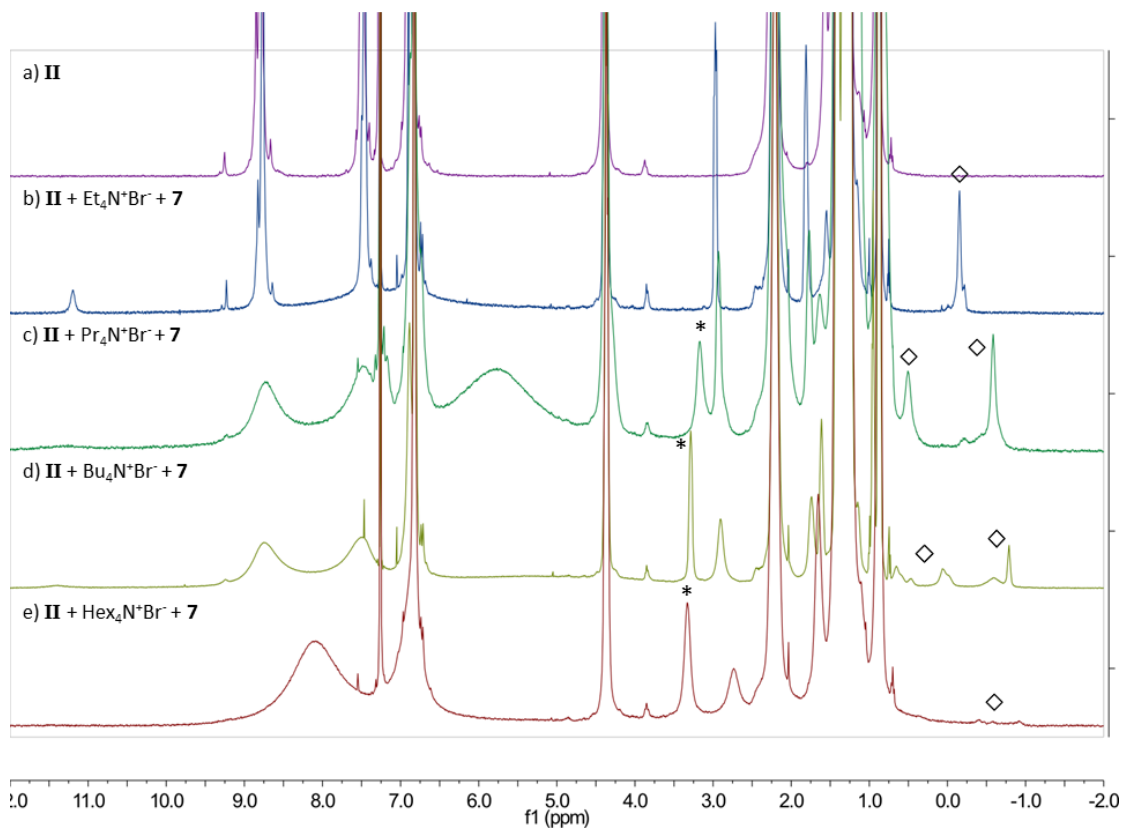
3.1 Comparison of tetraalkylammonium bromides (6a–d⁺Br⁻)



SI-Figure 4: Binding studies of resorcinarene capsule **I**. a) **I** (3.3 mM), with b) Et₄N⁺Br⁻ (**6a**⁺Br⁻) (3.3 mM); c) Pr₄N⁺Br⁻ (**6b**⁺Br⁻) (3.3 mM); d) Bu₄N⁺Br⁻ (**6c**⁺Br⁻) (3.3 mM); e) Hex₄N⁺Br⁻ (**6d**⁺Br⁻) (3.3 mM). Signals corresponding to free and encapsulated guest are highlighted by an asterisk and a square, respectively.



SI-Figure 5: Binding studies of pyrogallolarene capsule **II**. a) **II** (3.3 mM), with b) $\text{Et}_4\text{N}^+\text{Br}^-$ (**6a** $^+\text{Br}^-$) (3.3 mM); c) $\text{Pr}_4\text{N}^+\text{Br}^-$ (**6b** $^+\text{Br}^-$) (3.3 mM); d) $\text{Bu}_4\text{N}^+\text{Br}^-$ (**6c** $^+\text{Br}^-$) (3.3 mM); e) $\text{Hex}_4\text{N}^+\text{Br}^-$ (**6d** $^+\text{Br}^-$) (3.3 mM). Signals corresponding to free and encapsulated guest are highlighted by an asterisk and a square, respectively.



SI-Figure 6: Binding studies of pyrogallolarene capsule **II**. a) **II** (3.3 mM), with b) $\text{Et}_4\text{N}^+\text{Br}^-$ (**6a**⁺ Br^-) and trioctadecylamine (**7**), both (3.3 mM); c) $\text{Pr}_4\text{N}^+\text{Br}^-$ (**6b**⁺ Br^-) and **7**, both (3.3 mM); d) $\text{Bu}_4\text{N}^+\text{Br}^-$ (**6c**⁺ Br^-) and **7**, both (3.3 mM); e) $\text{Hex}_4\text{N}^+\text{Br}^-$ (**6d**⁺ Br^-) and **7**, both (3.3 mM). Signals corresponding to free and encapsulated guest are highlighted by an asterisk and a square, respectively.

3.2 Investigations concerning the precipitate formed with Et₄N⁺Br⁻ (**6a**⁺Br⁻)

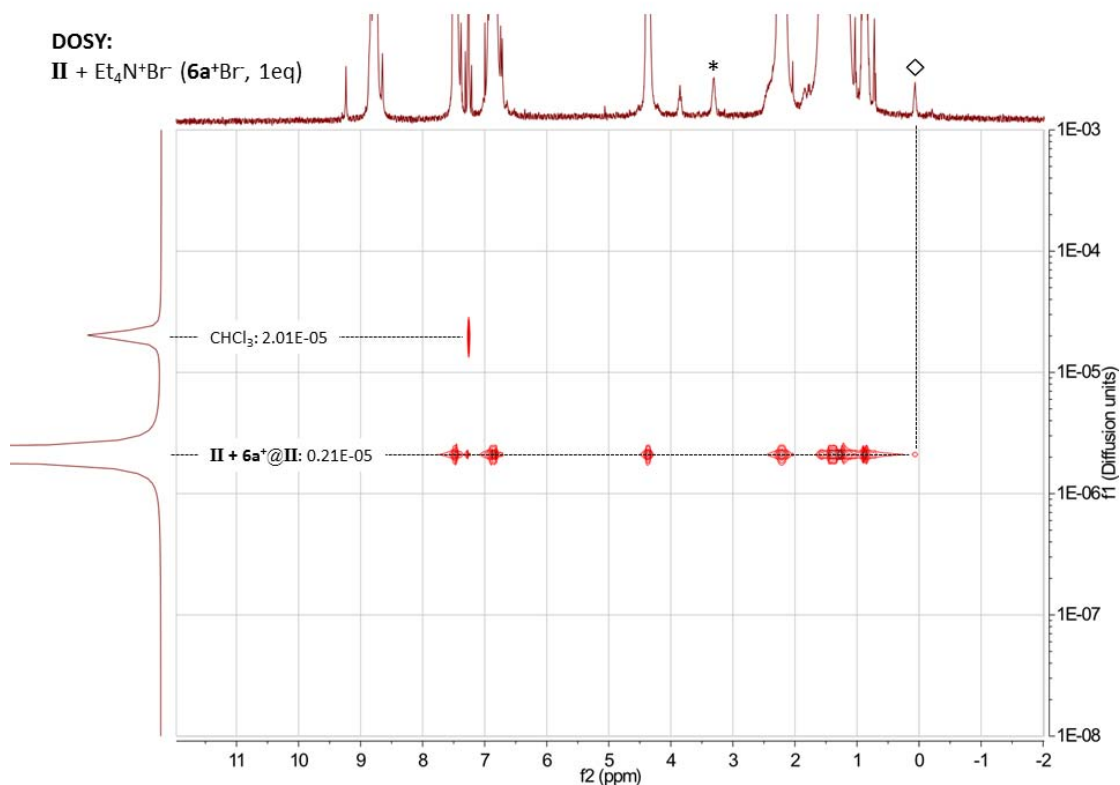
In the binding studies of **II** with Et₄N⁺Br⁻(**6a**⁺Br⁻) a precipitate formed. To clarify the reason for precipitate formation, samples of different **2/6a**⁺Br⁻-ratios (see *SI-Table 3*) were prepared with tetraethylsilane (Et₄Si, **9**) as an internal standard (SiCH₂, 0.53 ppm, q, *J* = 7.9 Hz, 8H). The amount of precipitate increased with time. The samples were measured 48h after preparation.

SI-Table 3: Investigation of the precipitation with Et₄N⁺Br⁻(**6a**⁺Br⁻) and **II**.

sample	2:6a ⁺ Br ⁻ : 9	2	Δ 2	6a ⁺ Br ⁻ (free+encap.)	Δ 6a ⁺ Br ⁻	Δ 2 : Δ 6a ⁺ Br ⁻
1	6:0:1	1.00eq	—	—	—	—
2	0:1:1	—	—	1.00eq	—	—
3	6:2:1	4.14eq	1.86eq	(0.70+0.37)eq	0.93eq	2.00:1
4	6:4:1	2.94eq	3.06eq	(2.05+0.44)eq	1.51eq	2.03:1
5	6:6:1	1.68eq	4.32eq	(3.37+0.47)eq	2.16eq	2.00:1

Using Et₄Si as reference, the decrease in pyrogallolarene **2** and **6a**⁺Br⁻ was determined by comparing the corresponding integrals with the ones of sample 1 and sample 2 (*SI-Table 3*). These experiments revealed a 2:1 stoichiometry of **2** and **6a**⁺Br⁻ in the precipitate and suggest that a dimer complex (**6a**⁺Br⁻@**2**₂) was formed as precipitate. Dimeric assemblies of pyrogallolarene (with shorter alkyl feet) containing ammonium species were previously observed in the solid state.⁴ A DOSY-experiment confirmed the integrity of **II** as a hexameric assembly in solution when encapsulating **6a**⁺Br⁻ (*SI-Figure 7*).

The equilibrium between hexameric and dimeric pyrogallolarene capsule is obviously driven to the dimeric species by precipitation. By employing a more bulky guest such as tetrapropylammonium bromide ($6b^+Br^-$), precipitation was completely suppressed.

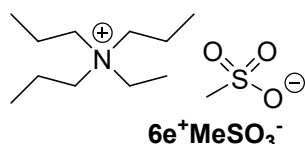


SI-Figure 7: DOSY spectrum of pyrogallolarene capsule **II** (3.3 mM) with $Et_4N^+Br^-$ ($6a^+Br^-$). The diffusion coefficients are given in cm^2/s . $II/6a^+Br^- = 1/1$. Signals corresponding to free and encapsulated guest are highlighted by an asterisk and a square, respectively.

3.3 Encapsulation studies with ethyltripropylammonium mesylate ($6e^+MeSO_3^-$)

The ammonium salt ($6e^+MeSO_3^-$) was selected to probe the location of the anion during encapsulation for the following reasons: (1) The medium size of cation $6e^+$ (between $6a^+$ and $6b^+$) not only efficiently prevents the formation of precipitate associating with the dimeric capsule of **2**, but also yields a reasonable encapsulation ratio for the binding study. (2) Compared to the original counterion Br^- , $MeSO_3^-$ is detectable by 1H - and ^{13}C -NMR spectroscopy, and among the available organic counterions, best resembles the Br^- in the term of the acidity of the corresponding conjugated acids.

3.3.1 Synthesis of ethyltripropylammonium mesylate ($6e^+MeSO_3^-$)



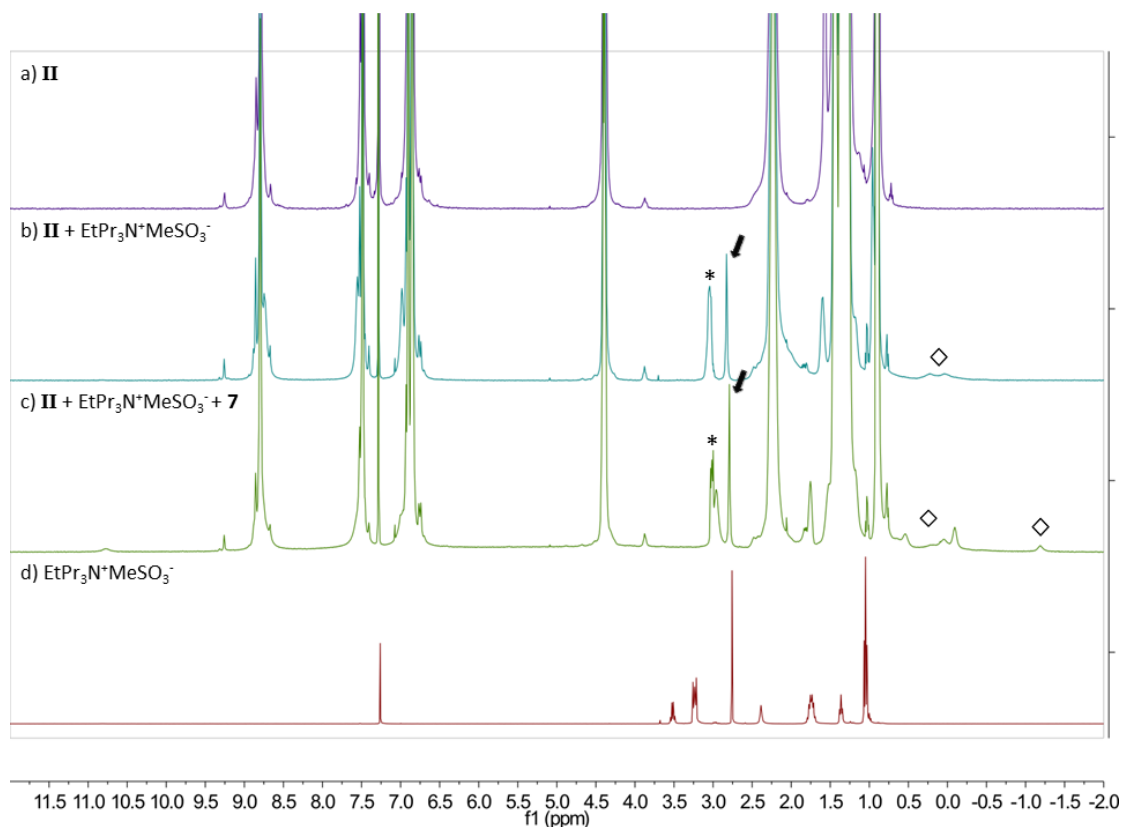
A mixture of ethyl methanesulfonate (0.17 mL, 1.6 mmol, 1.0 eq) and tripropylamine (1.52 mL, 8.0 mmol, 5.0 eq) was stirred in a pressure tube at 60 °C. After 24 h, the mixture was allowed to cool to rt and all volatile compounds were evaporated under reduced pressure (4 mbar) at 50 °C. The residue was washed with Et_2O (3x), to give the product (91 mg, 21%) as a pale yellow wax.

1H NMR (500 MHz, $CDCl_3$): δ 3.53 (q, $J = 7.2$ Hz, CH_2CH_3 , 2H), 3.28 – 3.19 (m, $CH_2CH_2CH_3$, 6H), 2.76 (s, $MeSO_3^-$, 3H), 1.79 – 1.70 (m, $CH_2CH_2CH_3$, 6H), 1.37 (t, $J = 7.2$ Hz, CH_2CH_3 , 3H), 1.05 (t, $J = 7.3$ Hz, $CH_2CH_2CH_3$, 9H).

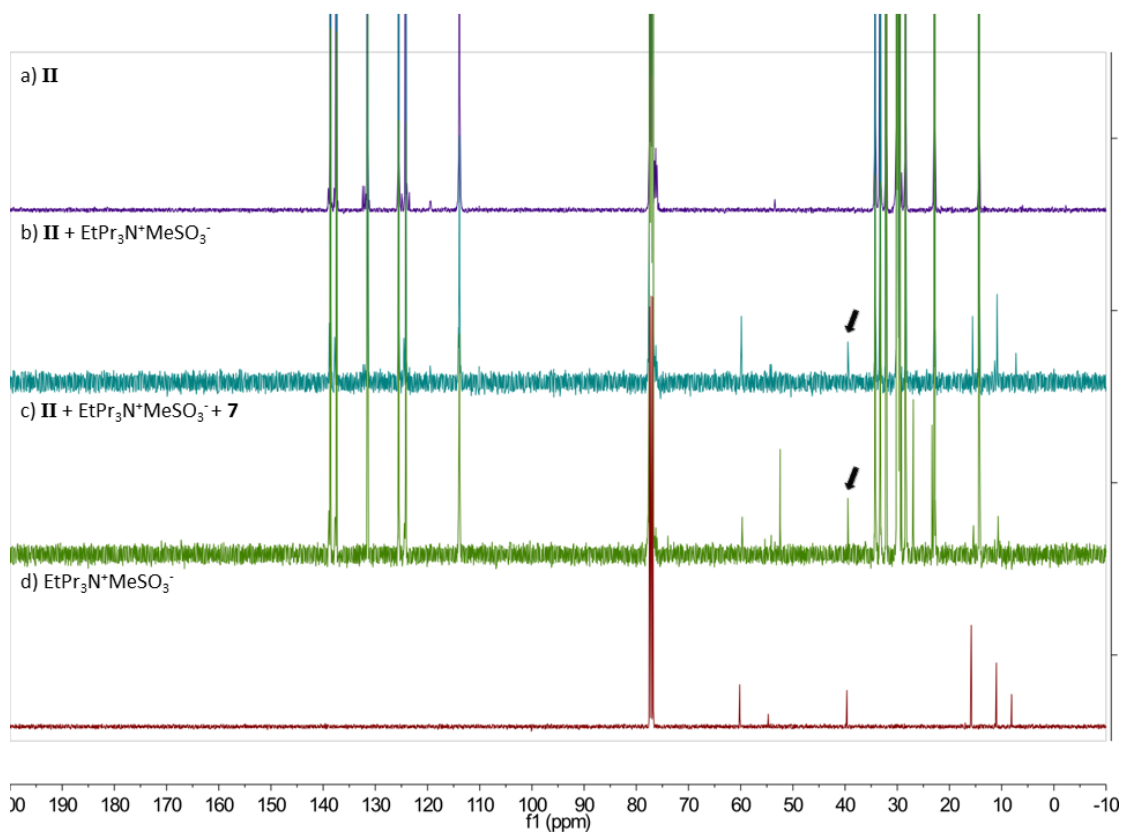
^{13}C NMR (126 MHz, $CDCl_3$): δ 60.2 ($CH_2CH_2CH_3$), 54.7 (CH_2CH_3), 39.7 ($MeSO_3^-$), 15.8 ($CH_2CH_2CH_3$), 11.0 ($CH_2CH_2CH_3$), 8.1 (CH_2CH_3).

IR (ATR): $\tilde{\nu}$ (cm^{-1}) = 3447, 2974, 1186, 1039, 768.

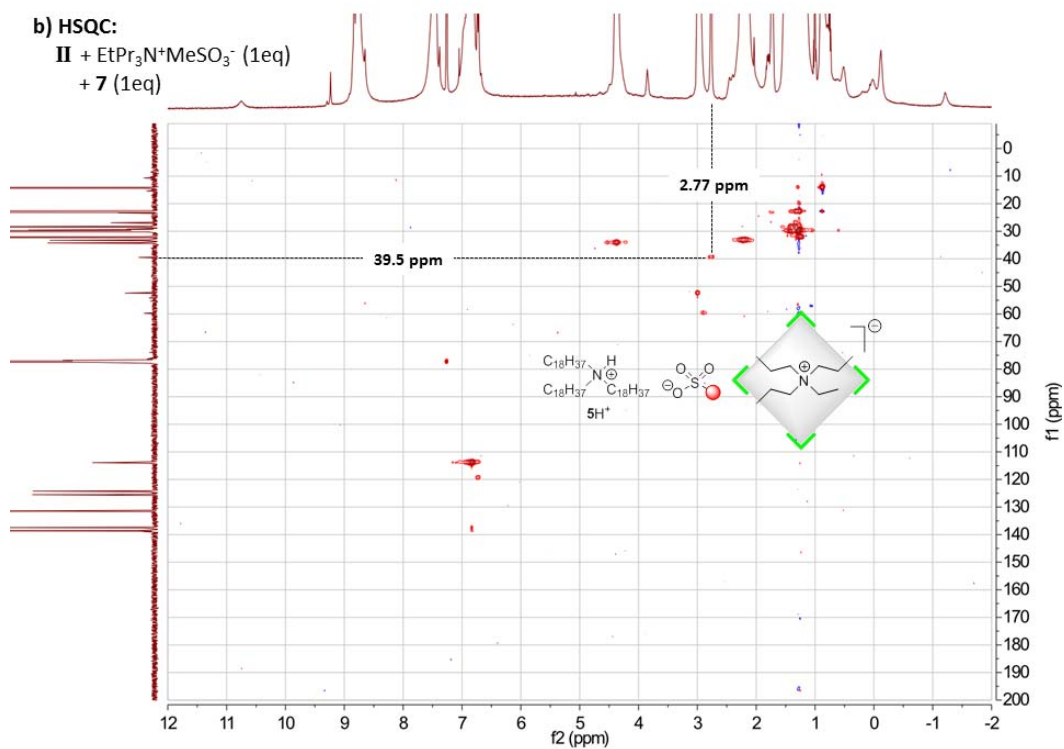
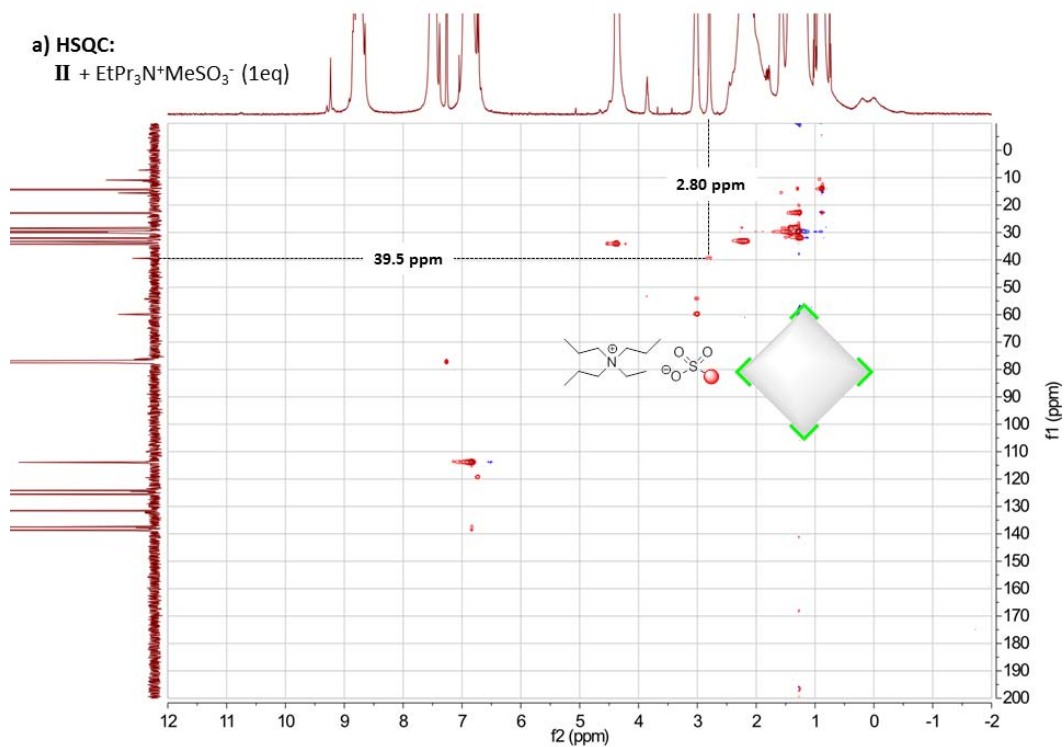
3.3.2 Binding studies



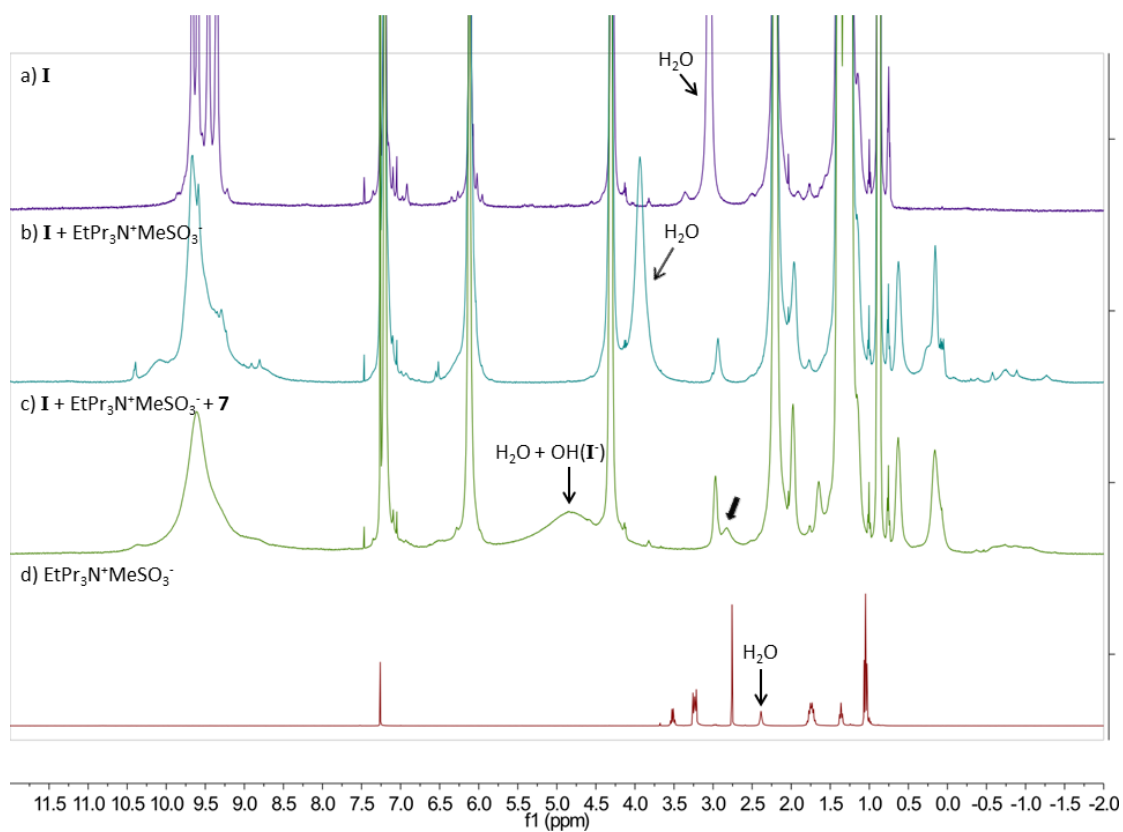
SI–Figure 8: Binding studies (^1H -NMR) of pyrogallolarene capsule **II**. a) **II** (3.3 mM), with b) $\text{EtPr}_3\text{N}^+\text{MeSO}_3^-$ (3.3 mM), integral of MeSO_3^- : 2.99 ± 0.03 H; c) $\text{EtPr}_3\text{N}^+\text{MeSO}_3^-$ and trioctadecylamine (**7**), both (3.3 mM), integral of MeSO_3^- : 3.04 ± 0.01 H; d) only $\text{EtPr}_3\text{N}^+\text{MeSO}_3^-$ (3.3 mM). Signals of free guest are highlighted by an asterisk (methylene groups adjacent to N-atoms) and an arrow (MeSO_3^-). Signals of encapsulated guest are highlighted by a square.



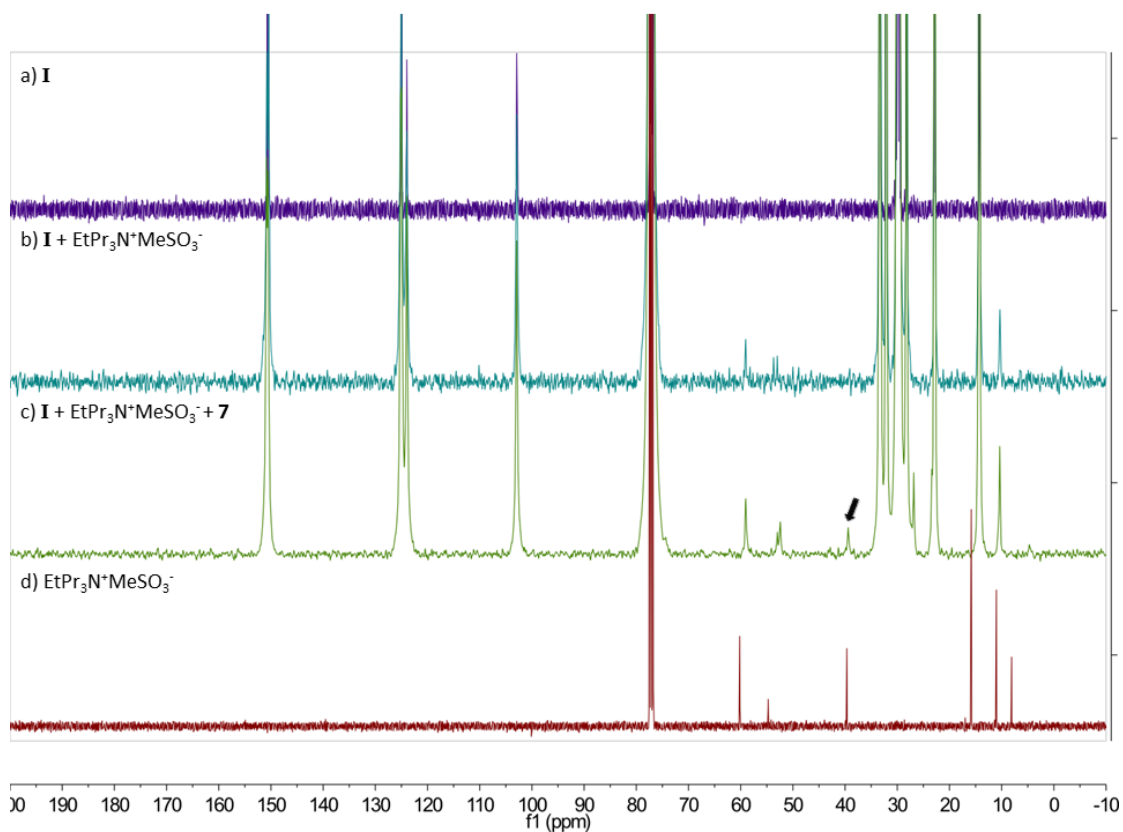
SI–Figure 9: Binding studies (^{13}C -NMR) of pyrogallolarene capsule **II**. a) **II** (3.3 mM), with b) $\text{EtPr}_3\text{N}^+\text{MeSO}_3^-$ (3.3 mM); c) $\text{EtPr}_3\text{N}^+\text{MeSO}_3^-$ and trioctadecylamine (**7**), both (3.3 mM). d) only $\text{EtPr}_3\text{N}^+\text{MeSO}_3^-$ (3.3 mM). Signal of free mesylate is highlighted by an arrow.



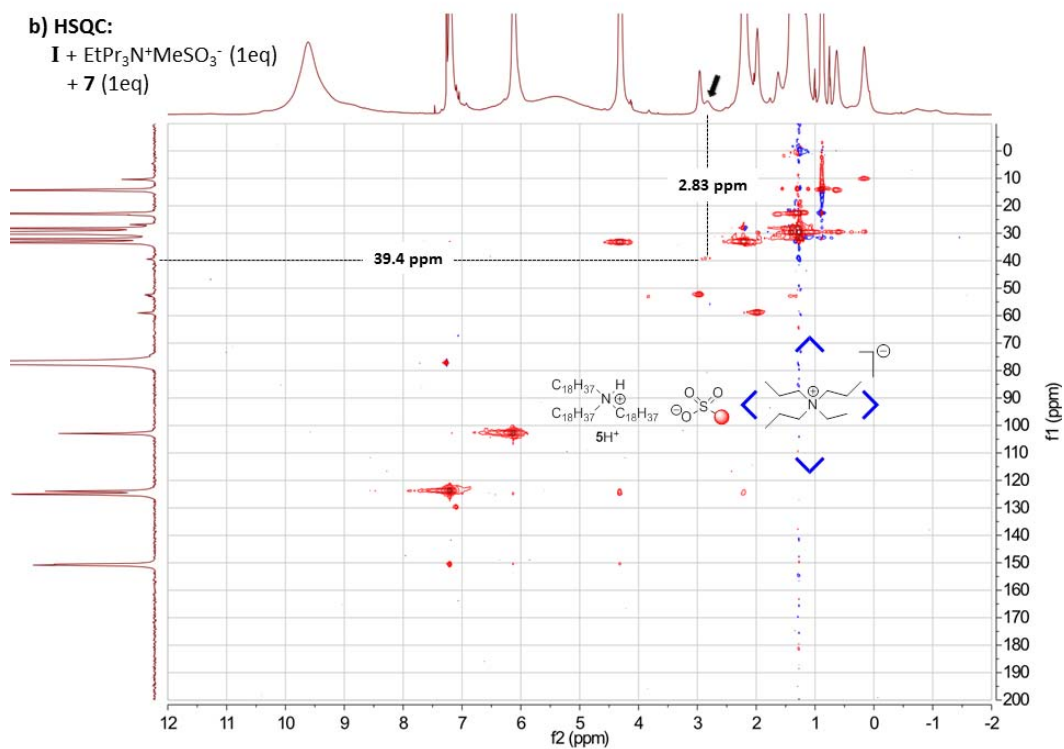
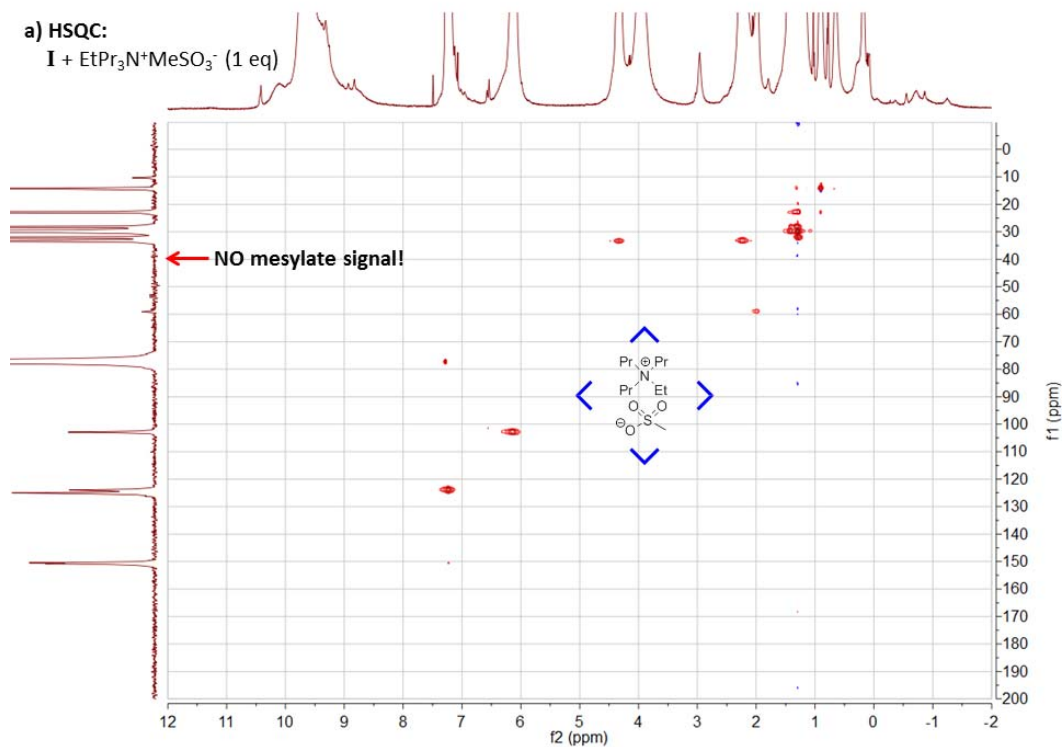
SI–Figure 10: HSQC spectra of pyrogallolarene capsule **II** (3.3 mM), with a) EtPr₃N⁺MeSO₃⁻ (3.3 mM); b) EtPr₃N⁺MeSO₃⁻ and trioctadecylamine (**7**), both (3.3 mM). Cross peaks of the mesylate group are highlighted.



SI-Figure 11: Binding studies (¹H-NMR) of resorcinarene capsule **I**. a) **I** (3.3 mM), with b) EtPr₃N⁺MeSO₃⁻ (3.3 mM), the signal of encapsulated MeSO₃⁻ is not visible due to peak overlap; c) EtPr₃N⁺MeSO₃⁻ and trioctadecylamine (**7**), both (3.3 mM); d) only EtPr₃N⁺MeSO₃⁻ (3.3 mM). Signal of the free mesylate is highlighted by an arrow.



SI-Figure 12: Binding studies (^{13}C -NMR) of resorcinarene capsule **I**. a) **I** (3.3 mM), with b) $\text{EtPr}_3\text{N}^+\text{MeSO}_3^-$ (3.3 mM); c) $\text{EtPr}_3\text{N}^+\text{MeSO}_3^-$ and trioctadecylamine (**7**), both (3.3 mM). d) only $\text{EtPr}_3\text{N}^+\text{MeSO}_3^-$ (3.3 mM). Signal of the free mesylate is highlighted by an arrow.

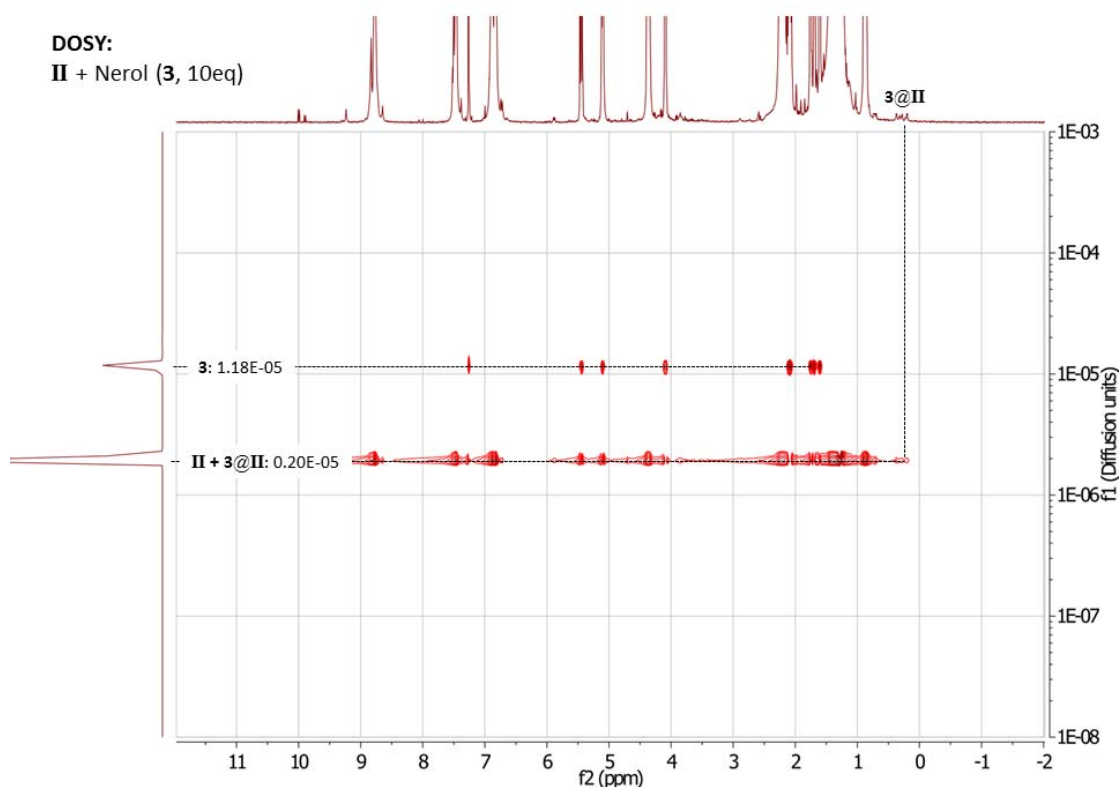


SI – Figure 13: HSQC spectra of resorcinarene capsule **I** (3.3 mM) with a) EtPr₃N⁺MeSO₃⁻ (3.3 mM); b) EtPr₃N⁺MeSO₃⁻ and trioctadecylamine (**7**), both (3.3 mM). Cross peaks of the mesylate group are highlighted.

4. Catalysis attempts with pyrogallolarene capsule II

4.1 Procedure for cyclization reactions

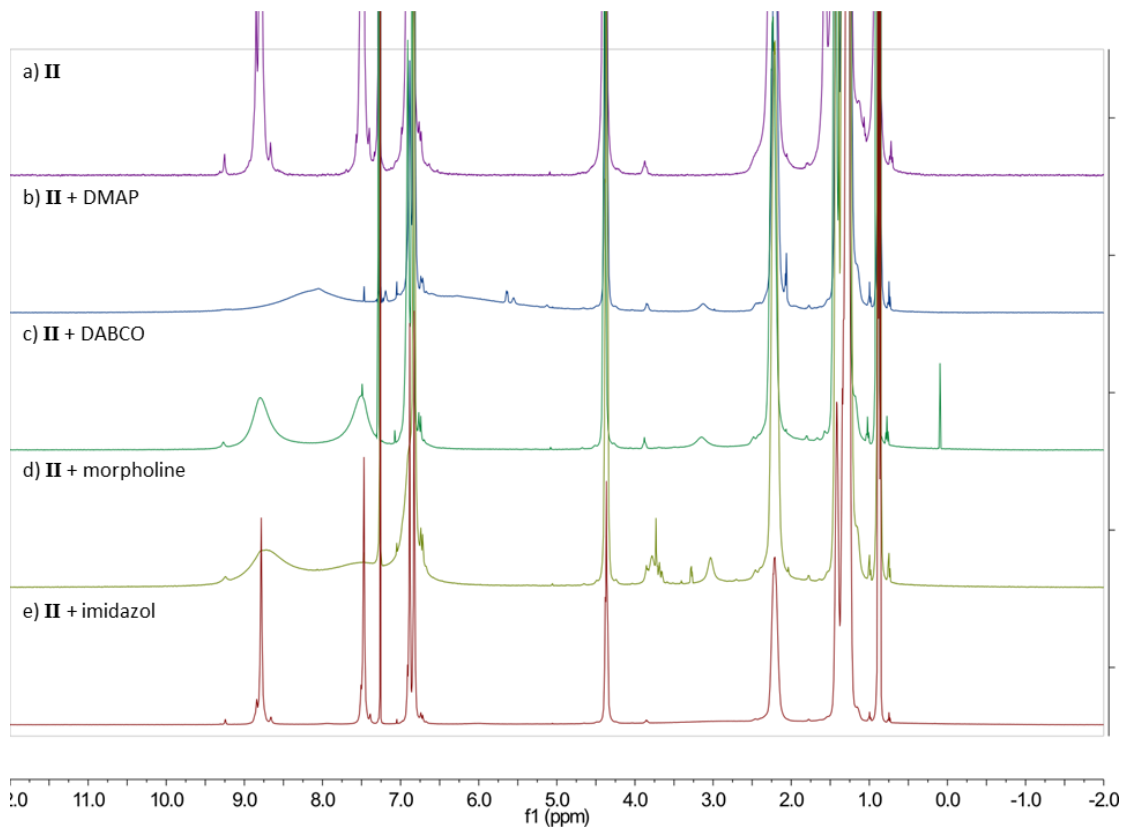
To a solution of substrate (2.9 μL nerol (**6**), 16.7 μmol , 10.0 eq) in 0.48 mL CDCl_3 was added *n*-decane stock solution in CDCl_3 (20 μL , 167 mmol/L, 3.34 μmol , 2.0 eq). At this point, a sample (approx. 10 μL) was diluted with 0.2 mL *n*-hexane and subjected to GC analysis (initial sample). Afterwards, pyrogallolarene capsule **II** (11.7 mg, 1.67 μmol , 1.0 eq) was added and the reaction was kept at 30 $^\circ\text{C}$. After 1 d, 2 d and 3 d, the reaction was sampled as described above and analyzed by GC. Although DOSY-experiment confirmed the encapsulation of substrate by capsule **II**, less than 5% conversion and no formation of cyclized terpene products could be detected after 3 d.



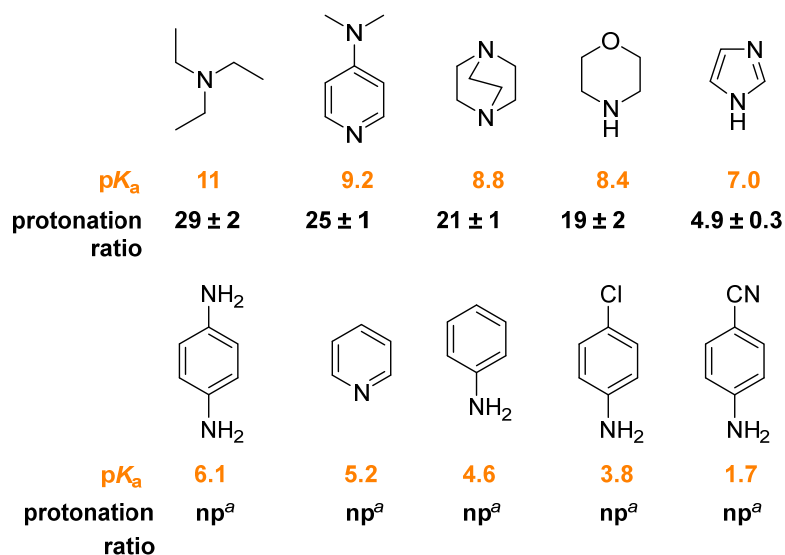
SI-Figure 14: DOSY spectrum of pyrogallolarene capsule **II** (3.3 mM) with nerol (**6**) (33 mM). The diffusion coefficients are given in cm^2/s .

4.2 Determination of the pK_a value of pyrogallolarene **II**

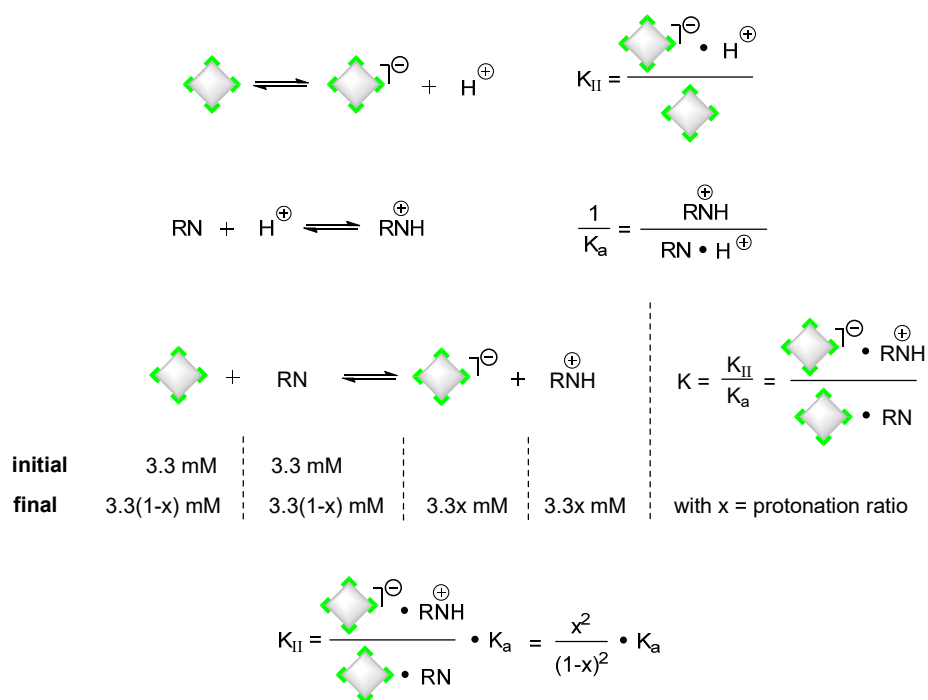
The acidity of hexamer **II** was determined in analogy to **I**,² by a series of protonation experiments with amines of varying basicity.



SI-Figure 15: ¹H-NMR spectra of pyrogallolarene capsule **II**. **a)** **II** (3.3 mM), with **b)** DMAP (3.3 mM); **c)** DABCO (3.3 mM); **d)** morpholine (3.3 mM); **e)** imidazole (3.3 mM).



^a np = no protonation detectable



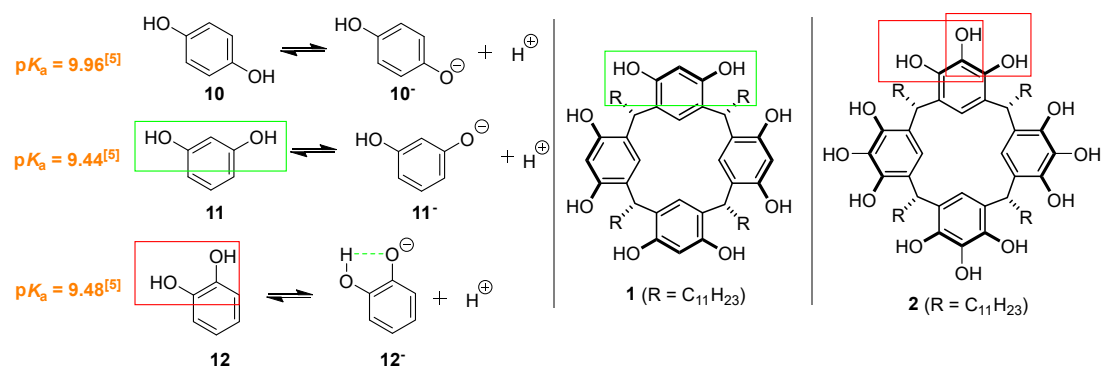
$$K_{\text{II}} = \frac{[\text{II}^{\ominus}] \cdot [\text{RNH}^{\oplus}]}{[\text{II}] \cdot [\text{RN}]} \cdot K_{\text{a}} = \frac{x^2}{(1-x)^2} \cdot K_{\text{a}}$$

	pK _a	deprotonation ratio of II	pK _{II}
DMAP	9.2	25±1%	10.2±0.1
DABCO	8.8	21±1%	10.0±0.03
Morpholine	8.4	19±2%	9.7±0.1
Imidazol	7.0	4.9±0.3%	9.6±0.1

SI-Figure 16: Estimation of the pK_a value of **II** by addition of 1.0 eq. of base to a solution of **II** in CDCl₃ (3.3 mM); SD from three independent experiments are given; pK_a values (measured in water) were taken from literature.⁵ The pK_a was estimated to be between 9.5 and 10.

Capsule **II** displayed a lower degree of deprotonation, as compared to capsule **I**. Bases with a pK_a -value ranging from 11 to 8.4, caused deprotonation ratios ranging from 29% to 19% (**Table 1a** in manuscript and **SI-Figure 16**). The deprotonation ratio dropped to 5% with imidazole ($pK_a = 7$). Weaker bases employed, failed to cause any deprotonation. Based on these results, the pK_a -value of capsule **II** was determined to be between 9.5 and 10 (ca. four pK_a units higher than resorcinarene capsule **I**).

The surprising acidity difference of **I** and **II** may arise from mesomeric destabilization (SI-Fig. 17).⁶ The pK_a value for hydroquinone (**10**) (benzene-1,4-diol) is considerably higher (ca. 0.5 pK_a units) than from benzene-1,3-diol (**11**), due to mesomeric destabilization of the phenolate. Benzene-1,3-diol (**11**) is even slightly more acidic than **12**, although the negative charge is stabilized by hydrogen bonding in **12**⁻. This further highlights the mesomeric destabilization of a phenolate by an *ortho* hydroxy group. The mesomeric destabilization (ca. 0.5 pK_a units) might well be multiplied in capsule **II**, due to the high number of destabilizing groups in *ortho*-positions, and therefore may explain the big difference in acidity between **I** and **II** (ca. four pK_a units).



SI-Figure 17: Mesomeric destabilization of phenolate anions by *ortho*- and *para*-hydroxy groups.

4.3 Catalysis attempts with additional external acids

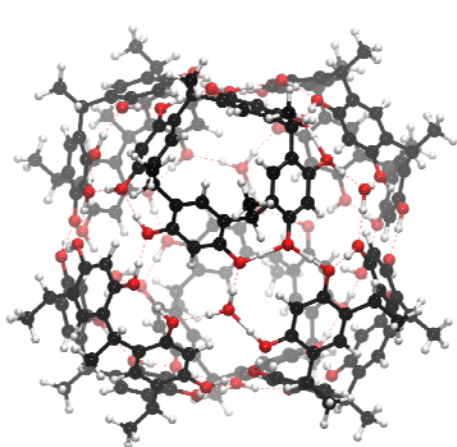
Since the failed activation of the substrate *via* protonation by **II** is the likely cause of its catalytic incompetence, we tried to initiate the cyclization reaction within **II**, by the addition of external stronger acids (10 mol% methanesulfonic acid or trifluoroacetic acid; 50 mol% *o*-nitrobenzoic acid, benzoic acid, *p*-nitrophenol or phenol). However, no difference to the background reaction (caused by added external acid) was detectable, indicating that the reaction only took place outside of **II**.

5. Quantum chemical calculations

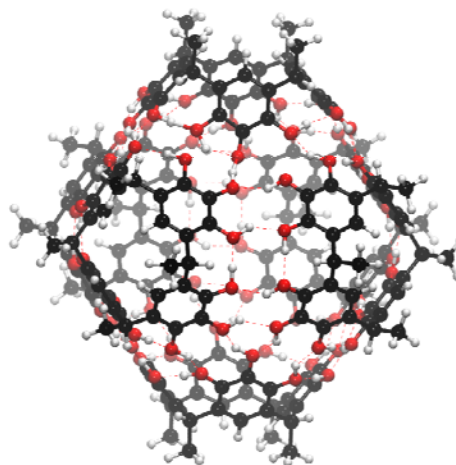
The structures of resorcinarene (capsule **I**) and pyrogallolarene (capsule **II**) hexamers with 455-486 atoms were optimized at the density functional theory (DFT) level using the dispersion corrected PBE-D3 functional,⁷ the multipole accelerated resolution of identity (RI-MARIE) approximation,⁸ and def2-SVP basis sets.⁹ The optimizations were performed with and without triethylamine in its protonated (HNEt₃⁺) and neutral (NEt₃) forms, as well as with tetraethylammonium (NEt₄⁺) and its salt (NEt₄⁺Br⁻) using the X-ray structures of the respective empty capsules as starting points. Solvation effects were treated using the conductor like-screening model (COSMO)¹⁰ to model the dielectric screening of trichloromethane with an ϵ set to 4.81. Binding affinities of the tetraalkylammonium species in **I** and **II** were also probed at PBE-D3/def2-TZVP level and using different density functionalities (PBE0-D3,¹¹ TPSS-D3,¹² B3LYP-D3.¹³ All quantum chemical calculations were performed using TURBOMOLE v. 5.5-5.6.¹⁴ Visual Molecular Dynamics (VMD) was used for visualization.¹⁵

SI Table 4. Binding affinity difference of NEt₄⁺ (in kcal mol⁻¹) with and without a halogen anion in capsules **I** and **II** at different density functional theory levels. $\Delta E(\text{NEt}_4^+:\text{Br}^-)$ and $\Delta E(\text{NEt}_4^+)$ refer to the affinity difference between NEt₄⁺Br⁻ and NEt₄⁺ towards capsules **I** vs. **II**, respectively. A negative (positive) sign refers to an exergonic (endergonic) binding of NEt₄⁺ to cluster **I** in comparison to cluster **II**. The medium was modeled as $\epsilon=4.81$ in all calculations.

	$\Delta E(\text{NEt}_4^+\text{Br}^-)$	$\Delta E(\text{NEt}_4^+)$
PBE-D3/def2-SVP	-3.2	+10.6
PBE-D3/def2-TZVP	-8.8	+4.1
PBE0-D3/def2-SVP	-3.3	+10.6
B3LYP-D3/def2-SVP	-2.7	+12.1
TPSS-D3/def2-SVP	-3.5	+10.7

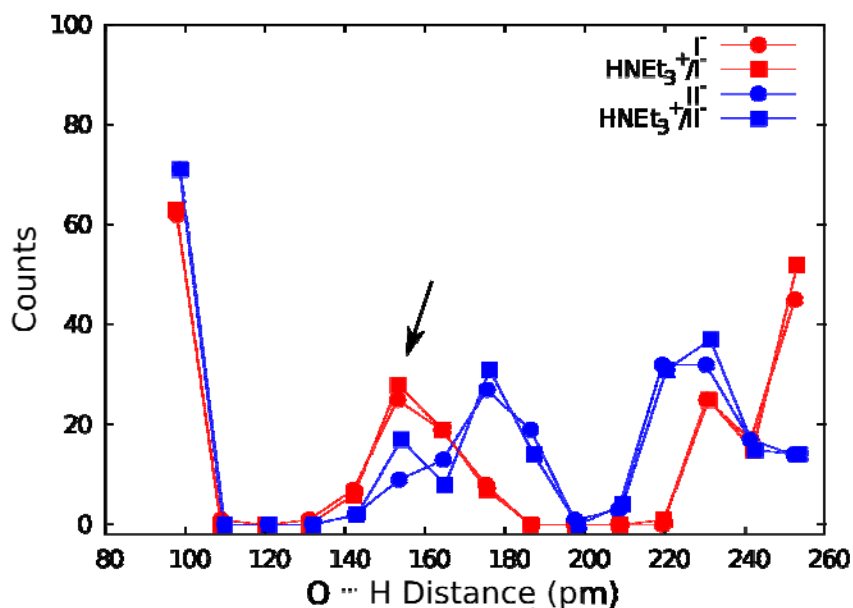


CI: $\text{PA}_{\text{rel}} = 0.0 \text{ kcal mol}^{-1}$



CII: $\text{PA}_{\text{rel}} = +4.7 \text{ kcal mol}^{-1}$

SI-Figure 18: DFT calculations at the PBE-D3/def2-SVP/ $\epsilon=4.81$ level of theory, suggesting that the relative proton affinity (PA) of **I** is *ca.* 5 kcal mol^{-1} lower than that of **II**. The PAs were estimated relative to the monomeric building blocks **1** and **2**.



SI-Figure 19: Distribution of O...H distances (in pm) in capsules **I** and **II** obtained

from PBE-D3/def2-SVP/ $\epsilon=4.81$ optimized structures. Delocalization of the anionic defect across several hydrogen bonds in **I** (red), while **II** shows a more localized defect (in blue). The delocalization of the anionic defect might lead to a lowering of the relative pK_a in capsule **I**.

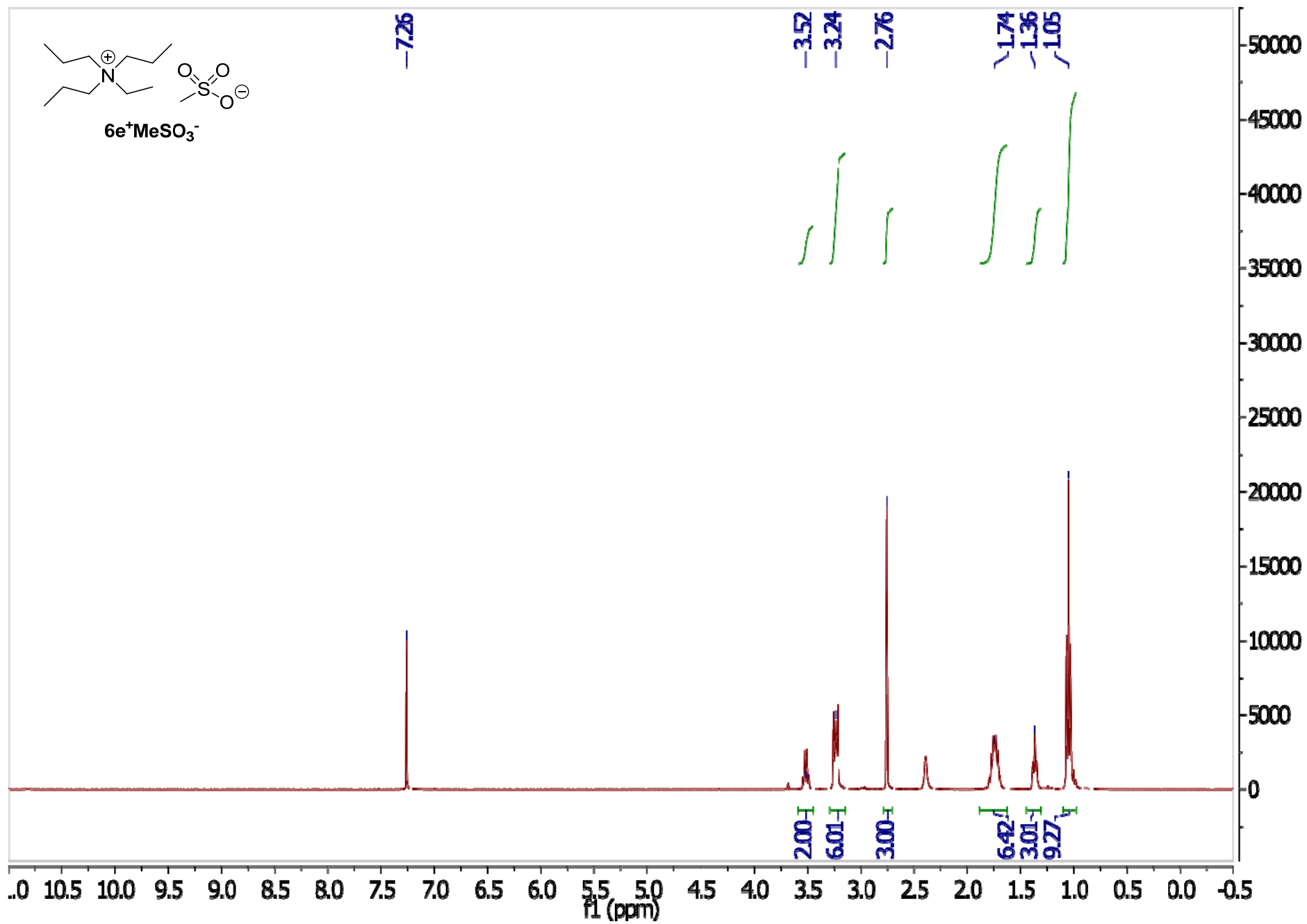
6. ESP surface map of capsule **I** and **II**

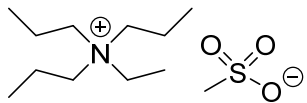
The ESP surfaces were calculated with Spartan '14 (Wavefunction, Irvine, CA, 2014, Version 1.1.8) at the AM1 level based on the DFT-optimized structures of **I** and **II**. It was reported, that the semi-empirical AM1 method produces reliable ESP surfaces.¹⁶ The potential energy values displayed in Fig. 3 of the manuscript, range from +104.6 kJ mol⁻¹ (25 kcal mol⁻¹) to -104.6 kJ mol⁻¹ (-25 kcal mol⁻¹). The red color indicates a value equal to or larger than the maximum in negative potential. The blue color indicates a value equal to or larger than the maximum in positive potential.

7. References

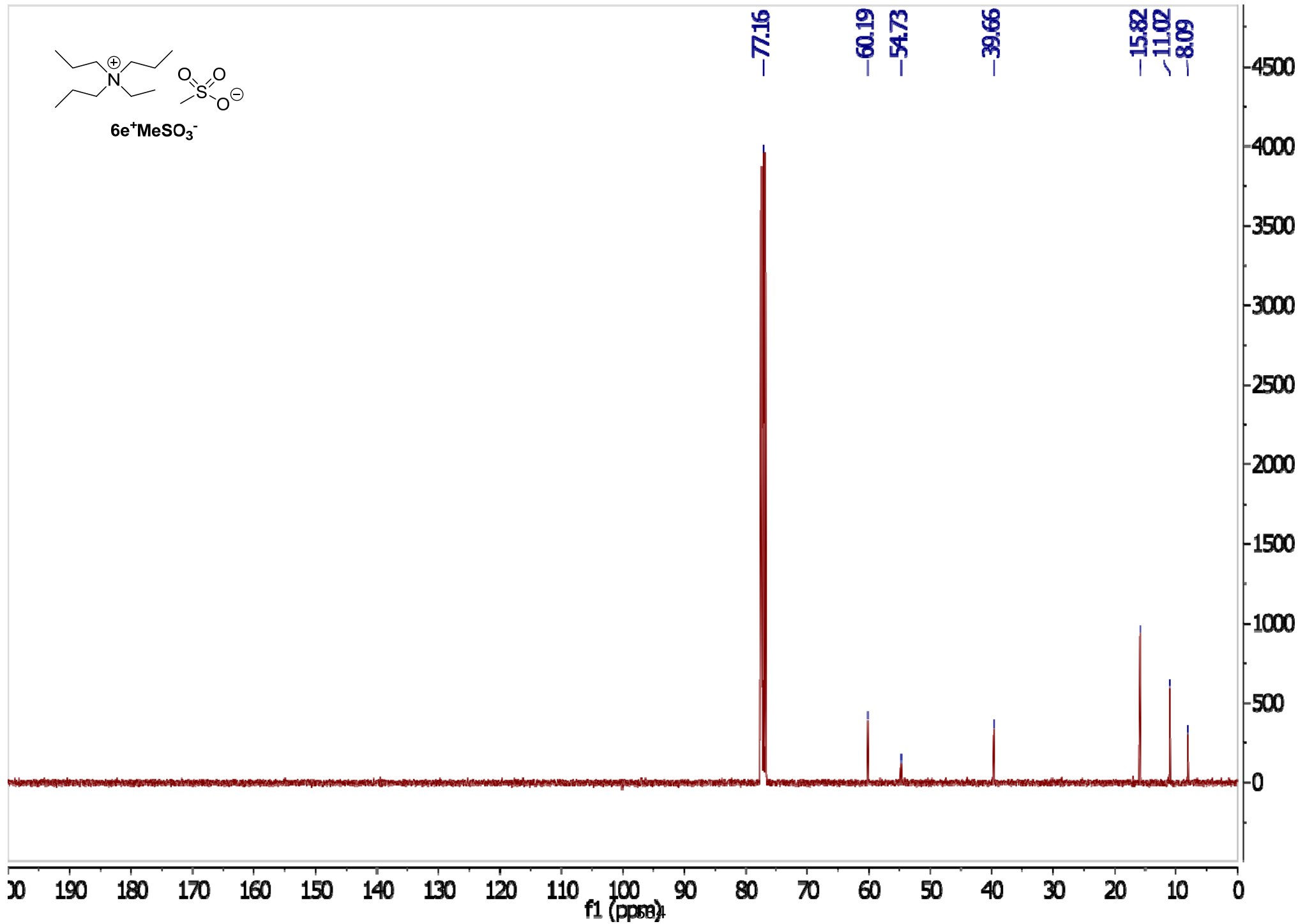
1. Zhang, Q.; Tiefenbacher, K., *Nature Chem.* **2015**, *7*, 197-202.
2. Zhang, Q.; Tiefenbacher, K., *J. Am. Chem. Soc.* **2013**, *135*, 16213-16219.
3. Letzel, M. C.; Agena, C.; Mattay, J., *J. Mass Spectrom.* **2002**, *37*, 63-68.
4. (a) Shivanyuk, A.; Friese, J. C.; Döring, S.; Rebek, J., *J. Org. Chem.* **2003**, *68*, 6489-6496; (b) Ahman, A.; Luostarinen, M.; Rissanen, K.; Nissinen, M., *New J. Chem.* **2007**, *31*, 169-177; (c) Beyeh, N. K.; Rissanen, K., *Isr. J. Chem.* **2011**, *51*, 769-780.
5. W. P. Jencks, J. R., *Ionization constants of acids and bases*. CRC Press: Cleveland, 1976; Vol. 1, p 305-351.
6. We thank Prof. Dr. Ulrich Lüning, Kiel University for this hypothesis.
7. (a) Perdew, J. P.; Burke, K.; Ernzerhof, M., *Phys. Rev. Lett.* **1996**, *77*, 3865-3868; (b) Grimme, S.; Antony, J.; Ehrlich, S.; Krieg, H., *J. Chem. Phys.* **2010**, *132*, 154104.
8. Sierka, M.; Hogeckamp, A.; Ahlrichs, R., *J. Chem. Phys.* **2003**, *118*, 9136-9148.
9. Weigend, F.; Ahlrichs, R., *Phys. Chem. Chem. Phys.* **2005**, *7*, 3297-3305.
10. Klamt, A.; Schuurmann, G., *J. Chem. Soc., Perkin Trans. 2* **1993**, 799-805.
11. Adamo, C.; Barone, V., *J. Chem. Phys.* **1999**, *110*, 6158-6170.
12. Tao, J.; Perdew, J. P.; Staroverov, V. N.; Scuseria, G. E., *Phys. Rev. Lett.* **2003**, *91*, 146401.
13. (a) Becke, A. D., *J. Chem. Phys.* **1993**, *98*, 5648-5652; (b) Lee, C.; Yang, W.; Parr, R. G., *Phys. Rev. B* **1988**, *37*, 785-789.
14. Ahlrichs, R.; Bär, M.; Häser, M.; Horn, H.; Kölmel, C., *Chem. Phys. Lett.* **1989**, *162*, 165-169.
15. Humphrey, W.; Dalke, A.; Schulten, K., *J. Mol. Graphics* **1996**, *14*, 33-38.
16. Mecozzi, S.; West, A. P.; Dougherty, D. A., *Proc. Natl. Acad. Sci. USA* **1996**, *93*, 10566-10571.

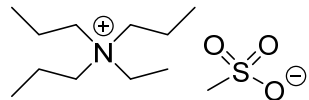
8. NMR spectra for new compounds





6e⁺MeSO₃⁻





6e⁺MeSO₃⁻

